

MAADLY Spanning the Length Scales in Dynamic Fracture

Farid F. Abraham¹

Abstract: A challenging paradigm in the computational sciences is the coupling of the continuum, the atomistic and the quantum descriptions of matter for a *unified dynamic* treatment of a single physical problem. We described the achievement of such a goal. We have *spanned the length scales* in a concerted simulation comprising the finite-element method, classical molecular dynamics, quantum tight-binding dynamics and seamless bridges between these different physical descriptions. We illustrate and validate the methodology for crack propagation in silicon.

1 Introduction

The traditional approach to *coupling length and time scales* is to solve a problem in a serial fashion by doing one set of calculations at a very fundamental level, and of high computational complexity, and use the results to evaluate constants in a more approximate or phenomenological computational methodology at a longer length/time scales. An example is the pioneering work of Clementi and coworkers [Clementi (1988)] in the 1980s where they used quantum mechanics, atomistic dynamics, and fluid dynamics to predict the tidal circulation in Buzzard's Bay Massachusetts: in a series of calculations, each calculation was used as input to the next up the length and time hierarchy. There are many examples in the literature where an appropriate computational methodology is used for a given scale or task, whether it be the accuracy of quantum mechanics at the shortest scales, or the approximation of continuum mechanics at the longest scales. In contrast, there has been comparatively little effort devoted to the parallel coupling of different computational schemes for a simultaneous attack on a given problem. We will present such an effort where our interest concerns issues in materials physics.

This challenging paradigm of computational science demands a *unified dynamical* treatment of a physical problem. This requires the simultaneous use of the tools of engineering, physics and chemistry in a seamless formalism. We describe such an accomplishment for the study of brittle fracture in silicon, though our approach has general applicability. In a single concerted simulation of dynamic fracture comprising the finite-element method, classical molecular dynamics and quantum tight-binding dynamics, we demonstrate that *spanning the length scales* with dynamical bridges between the different physical descriptions is feasible. Our approach maps naturally onto scalable computer architectures.

The traditional approach for studying fracture is to adopt continuum mechanics [Cottrell (1964); Freund (1990)], the macroscopic view of matter. Because continuum mechanics allows material lengths to go to zero, there is no natural small-length cutoff, such as the size of an atom. Hence, a failure mechanism describing the loss of local material cohesion (e.g., void formation) does not arise naturally from this macroscopic description. At the finer level of description of classical atoms interacting through empirical force laws, material decohesion does arise naturally [Abraham, Brodbeck, Rafey, and Rudge (1994); Abraham, Schneider, Land, Lifka, Skovira, Gerner, and Rosendrantz (1997)], and we choose to label this length scale the atomic regime. We can even go one level finer. Treating bond breaking with an empirical potential may be unreliable, and a quantum mechanical treatment may be desired. This *abinitio* level of description we call the quantum regime. And if the crack is moving, a unified macroscopic, atomistic, abinitio dynamics (MAAD) description must be brought together into a seamless union, embracing all of the size-scales, from the very small to the very big. We do not address the very important issue of spanning the time-scale.

I will describe an implementation of such a program. The original MAAD investigators were Jeremy Broughton, E. Kaxiris, N. Bernstein and the present author. This review follows one of our original papers [Abraham, Broughton, Bernstein, and Kaxiras (1998)] with the incorporation of later extensions and corrections [Broughton, Abraham, Berstein, and Kaxiras (1999); Abraham, Broughton, Berstein, and Kaxiras (1998); Abraham, Bernstein, Broughton, , and Hess (2000)]. Other recent studies describing a methods for interfacing the continuum and the atomistic regimes or the atomistic and the quantum regimes are given in Hoover, De Groot, and Hoover (1992); Rafii-Tabar, Hua, and Cross (1998); Shenoy, Miller, Tadmor, and Phillips (1998); Capaz, Cho, and Joannopoulos (1995); Vanduijnen and Devries (1996). We are unaware of any study coupling all three regimes either concurrently or dynamically.

2 The Spatial Decomposition - FE/MD/TB

Our MAAD simulation is composed of computational procedures formulated in terms of a spatial decomposition of the system and has an obvious applicability for parallel processing. Our application is the brittle fracture of a silicon slab flawed by a microcrack at its center and under uniaxial tension. Figure 4 shows the geometrical decomposition of the

¹ IBM Research Division, Almaden Research Center, San Jose, CA 95120

silicon slab into the five different dynamic regions of the simulation: the continuum finite-element region (FE); the atomistic molecular dynamics region (MD); the quantum tight-binding region (TB); the FE-MD *handshaking* region; and the MD-TB *handshaking* region. The image is the simulated silicon slab, with expanded views of the FE-MD (orange nodes-blue atoms) interface and the TB (yellow atoms) region surrounded by MD (blue) atoms. Note that the TB region surrounds the crack tip with broken-bond MD atoms trailing behind this region. Not all of the FE and MD regions are shown since their extent is large.

2.1 FE-Ingredients

In the "far-field" regions, we have a continuum treated by the well known finite-element (FE) procedure [Hughes (1987)]. This macroscopic description merely needs the constitutive law for the material. Details of the finite-element method are now given.

In the FE technique, the continuum elastic energy (which is a function of the displacement field, a continuous variable) is integrated over the entire volume of the sample by placing a mesh over the system. If the displacements are known at the mesh points (nodes), then interpolation can be used within each element (cell) of the mesh to determine the displacement field everywhere. The elastic energy integral is then replaced by a sum over cells (triangles in 2D, tetrahedra in 3D) and the important dynamical variables in the problem are the values of the displacements at the nodes. The kinetic energy integral is handled similarly. Since an energy is defined for the FE region, forces on the dynamical variables can be obtained. Thus the time evolution of the system may be propagated in the same way as MD. In the FE/MD handshake region it is important to have FE mesh points coincident with the ideal atomic sites of the MD region; thus it is academic whether we think of these sites as representing atoms or nodes. We itemize the key steps in the finite-element procedure.

- The Hamiltonian, without body forces or tractions, is defined by

$$E = \frac{1}{2} \int dV \varepsilon_{\mu\nu} C_{\mu\nu\lambda\sigma} \varepsilon_{\lambda\sigma} + \frac{1}{2} \int dV \rho |\dot{u}|^2$$

where ε is the strain tensor, C is the elastic constant matrix, ρ is the density and \dot{u} is the time derivative of the displacement field.

- The interpolation of a function within the finite element cell is defined by

$$f(x) = (A_1 f_1 + A_2 f_2 + A_3 f_3) / (A_1 + A_2 + A_3)$$

where f_i is the value of the function at node i and A_i is the corresponding area (as shown in the figure).

- Performing the integral over each cell yields the energy evaluated on the mesh

$$E = \sum_i^{\#cells} \left\{ \frac{1}{2} u_{\alpha}^i K_{\alpha\beta}^i u_{\beta}^i + \frac{1}{2} \dot{u}_{\alpha}^i M_{\alpha\beta}^i \dot{u}_{\beta}^i \right\}$$

where u^i is the displacement field at node i , and K and M are local stiffness and mass matrices that incorporate linear interpolation in each triangle.

- Since we have a Hamiltonian, we can advance through time in lock-step with MD using an identical integrator.

2.2 MD-Ingredients

Around the crack where large deformation occurs with no bond rupture, we use the classical molecular dynamic (MD) method to treat the highly nonlinear deformation on the atomic scale. Because MD has a large computational burden, we partition this region spatially onto several processors. Details of the molecular dynamics is now given.

In the MD technique, atoms are propagated through space and time using Newton's laws of motion. At most ambient temperatures and for most elements, a classical (as opposed to quantum) description of the dynamics of atomic motion is perfectly satisfactory. All that is required is an interatomic force law. For silicon, many force laws have been parameterized using equilibrium experimental observations. We chose the potential due to Stillinger and Weber (1985). They write the total potential energy of the system as a sum over pairs of atoms plus a sum over triplets of atoms. The pair sum represents bonds between atoms and is a function of their distance apart. The triplet sum describes bond bending terms and is a function of the angle between pairs of bonds centered on any given atom. In a covalent solid such as silicon, the bond bending terms are important; they are what differentiate the structural properties from those of a metal. Forces, required for the MD position update algorithm, are obtained from derivatives of the potential energy. We itemize the key steps in the molecular dynamics procedure.

- The Hamiltonian consists of the normal kinetic energy

$$E_k = \sum_i^{atoms} \frac{1}{2} m |v_i|^2$$

plus a potential energy defined by the function

$$E_p = \sum_{ij}^{pairs} V^{(2)}(r_{ij}) + \sum_{ijk}^{triplets} V^{(3)}(r_{ij}, r_{jk}, \theta_{ijk})$$

where r_{ij} is the distance between atoms i and j , θ_{ijk} is the angle between bonds $i-j$ and $j-k$, $V^{(2)}$ is the pair potential and $V^{(3)}$ is the three body potential.

- The equations of motion are integrated with respect to time using a multiple time step algorithm based on a Trotter expansion of the Liouville operator [Tuckerman, Berne, and Martyna (1990)].
- The code is parallelized using a 1D domain decomposition; data flows via 1D shift operator.

2.3 TB-Ingredients

Lastly, in the region of bond failure at the crack tip, we use the tight-binding (TB) formalism which is a semiempirical elec-

tronic structure description of matter. It is one of the fastest numerical quantum methods containing electronic structure information. Rather than evaluating costly integrals, it uses pre-determined parameterized matrix elements for the material under study. For this silicon study, we employ the nonorthogonal TB scheme due to Bernstein and Kaxiras (1997). The nuclei are treated as classical point objects. Because the TB region is the most computationally demanding part of the overall code, a small TB region must be used so as to allow overall load balancing. Details of the tight-binding method follow.

In the TB technique, the energy of the system is written as an eigenvalue sum plus interatomic pairwise terms. The eigenvalues are parameterized to be as close as possible to those of an abinitio quantum mechanical calculation. The sum is over occupied one electron states up to the Fermi level. The parameterization is of the elements which comprise the TB Hamiltonian matrix. This matrix has to be diagonalized at every time step of the simulation; i.e. for every configuration of atoms in the TB region. Since diagonalization is order N^3 computationally expensive, this is the most computationally complex part of the whole coupled algorithm. Each matrix element is a function of (a) the distance between pairs of atoms and (b) the basis function sitting on either site. Each silicon has one s and three p atomic basis orbitals. The other term in the total energy originates because, in ab-initio one-electron theories like Hartree-Fock or Density Functional Theory, the total energy is not just an eigenvalue sum: it has additional terms due to double counting of Coulomb integrals and exchange-correlation terms. To good approximation these can be parameterized via a pairwise sum. As with the FE and MD regions, forces are obtained from derivatives of the energy. The atoms in the TB region can be updated in lock-step with the rest of the system.

In the MD/TB handshake region, the surface dangling bonds of the embedded TB cluster are terminated with monovalent atoms: "silogens". These silogens are constrained to be coincident with the silicons of the inner perimeter the MD region. The coupling may therefore be envisaged as a TB cluster residing in an MD void but with the outer TB silogens sitting on top of the inner MD silicons. Careful book-keeping in the handshake region allows all bonds to be accounted for. Each silogen has a single s atomic basis orbital. The TB matrix is thus $(4N_{in} + N_{out})^2$ in size where N_{in} represents the number of silicons and N_{out} represents the number of silogens in each TB region. We itemize the key steps in the tight-binding procedure.

- The Hamiltonian consists of the same kinetic energy as for MD plus a potential energy defined by

$$E_p = \sum_n^{\#occ} \epsilon_n + \sum_{ij}^{pairs} \phi(r_{ij})$$

where ϵ_n is the eigenvalue of state n , the first sum is carried out over the occupied electronic states, and $\phi(r_{ij})$ is the pairwise interaction between atoms i and j .

- The eigenvalues are calculated by solving the matrix

equation

$$\mathbf{H}\Psi_n = \epsilon_n \mathbf{S}\Psi_n$$

where \mathbf{H} is the electronic Hamiltonian matrix, \mathbf{S} is the overlap matrix, and Ψ_n is the eigenvector of state n .

- The matrix elements

$$\begin{aligned} H_{lm} &= \langle \phi_l | \mathbf{H} | \phi_m \rangle \\ S_{lm} &= \langle \phi_l | \phi_m \rangle \end{aligned}$$

are computed within the two-center approximation and decay smoothly to zero at $r \Rightarrow r_c$.

- Solving the generalized eigenvalue problem yields the forces which are the expectation values of derivatives of \mathbf{H} and \mathbf{S} .
- The TB dynamics is advanced in lock-step with MD using same time integrator.

We track the path of the crack by placing the center of the TB region at the apex of the crack and along the line defining the forward direction of motion. In the approach discussed in our original study [Abraham, Broughton, Bernstein, and Kaxiras (1998)], a cluster of eight small TB subregions was used to speed up the calculations for the TB region, which is the most computationally demanding part of the overall code. We have since found that this overlapping TB cluster scheme is inaccurate and makes the TB region behave more like a region Stillinger-Weber atoms [Abraham, Bernstein, Broughton, , and Hess (2000)]. With the multicluster scheme, the TB crack tip and the SW crack tip had essentially identical dynamics. We now use a single TB cluster of atoms. Bernstein has developed a new method for computing the forces in the TB region that is presently computationally more expensive in practice but scales linearly with the number of atoms [Abraham, Bernstein, Broughton, , and Hess (2000)]. It was the results of Bernstein's method that led to the discovery that the original tight-binding multicluster approximation was inaccurate. We will not discuss Bernstein's method here, but it is discussed in Abraham, Bernstein, Broughton, , and Hess (2000).

2.4 FE/MD and MD/TB Handshaking

Two crucial aspects of our MAAD procedure are the handshaking algorithms between the FE and the MD and between the MD and the TB where *seamless* couplings are required [Abraham, Broughton, Bernstein, and Kaxiras (1998); Broughton, Abraham, Bernstein, and Kaxiras (1999); Abraham, Broughton, Bernstein, and Kaxiras (1998); Abraham, Bernstein, Broughton, , and Hess (2000)]. In the FE/MD handshake region (Figure 1), the FE mesh spacing is scaled to atomic dimensions. Moving away from the FE/MD region and deep into the continuum, we can expand the mesh size. Thus we can embed our atomistic simulation in a large continuum solid. FE cells contribute fully to overall the Hamiltonian (unit weight). FE cells contributing to handshake Hamiltonian

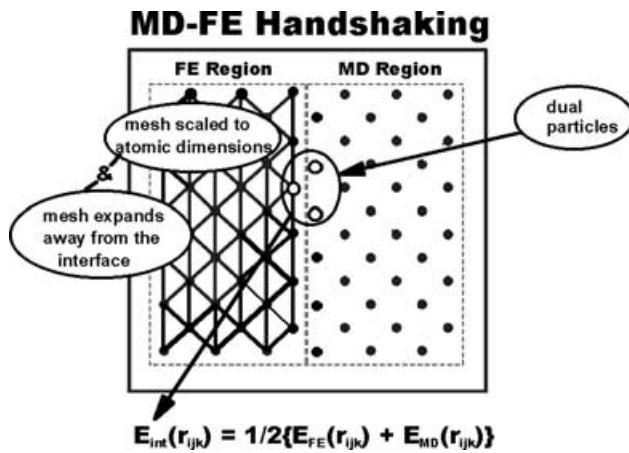


Figure 1 : Illustration of FE/MD handshake Hamiltonian (see text).

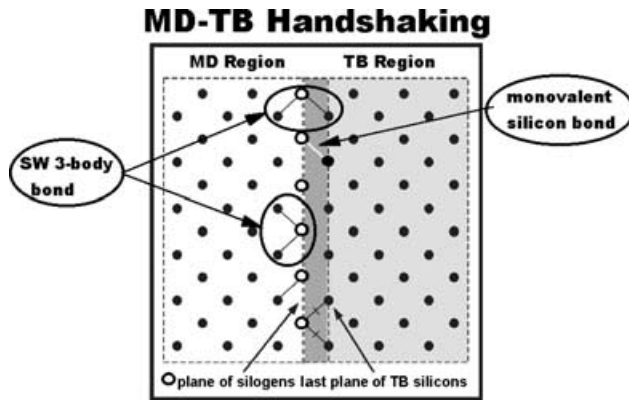


Figure 2 : Illustration of MD/TB handshake Hamiltonian (see text).

have half weight. Two and three body terms of SW interaction which cross boundary also carry half weight. The FE region has displacements associated with each mesh point which follow a Hamiltonian given by continuum linear elasticity theory. We employ an update algorithm identical to that used in conventional MD so that the displacements now are dynamical variables which follow in lock-step with those of their atomic cousins in the MD region. The FE/MD interface is chosen to be far from the fracture region; hence atoms and the displacements of the FE lattice can be unambiguously assigned to one another. This is accomplished by taking the interactions across the FE/MD boundary to be the mean of the FE Hookian description and the MD interatomic potential description.

For the MD/TB handshake interface (Figure 2), dangling bonds at the edge of the TB region are passivated with special terminating atoms. These are fictitious atoms that interact with the electrons of the silicon atoms at the surface of the region so as to tie off a single bond each, minimizing the effects of

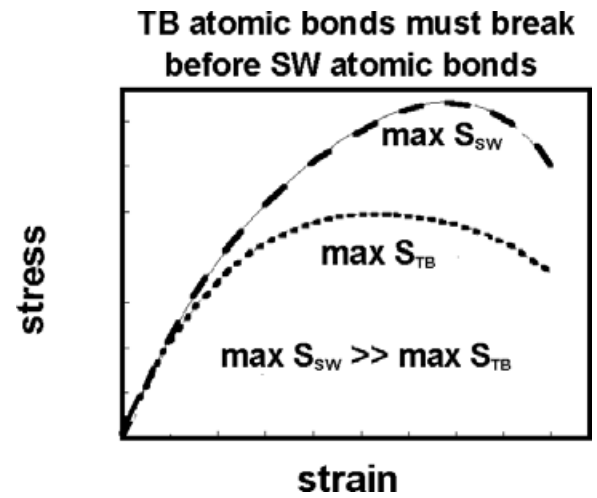


Figure 3 : Energy-strain and stress-strain relations for bulk silicon as predicted using Stillinger-Weber (SW) empirical potential and the Tight-Binding (TB) method.

the surface on the forces inside the cluster. The TB terminating atoms bond like silicon, but are monovalent like hydrogen, hence the name *silogens*. At the surface of the TB region we place silogens that sit directly on top of the atoms of the MD simulation. The SW force is computed for these boundary atoms considering only bonds to atoms in the MD region. The contribution from the missing bonds is accounted for by adding the force computed for each silogen to the atom it represents. As before, the atomic positions of the TB atoms are updated in lock step with their FE and MD cousins. The entire procedure is formulated in such a way that the simulation, in the absence of dynamic TB tracking of the crack front, conserves total energy. A detailed discussion of the MAAD techniques is given in Broughton, Abraham, Berstein, and Kaxiras (1999).

2.5 The Total System

For small deformations, overall consistency was ensured by making sure that the linear elastic constants in all three regions are the same.

A Hamiltonian, H_{Tot} , is defined for the entire system. Its degrees of freedom are atomic positions, \mathbf{r} , and their velocities, $\dot{\mathbf{r}}$, for the TB and MD regions; and displacements, \mathbf{u} , and their time rates of change, $\dot{\mathbf{u}}$, for the FE regions. (The velocities and conjugate momenta are simply related). Equations of motion for all the relevant variables in the system are obtained by taking the appropriate derivatives of this Hamiltonian. All variables can then be updated in lock-step as a function of time using the same integrator. Thus the entire time history of the system may be obtained numerically given an appropriate set of initial conditions. Conceptually, H_{Tot} may be written:

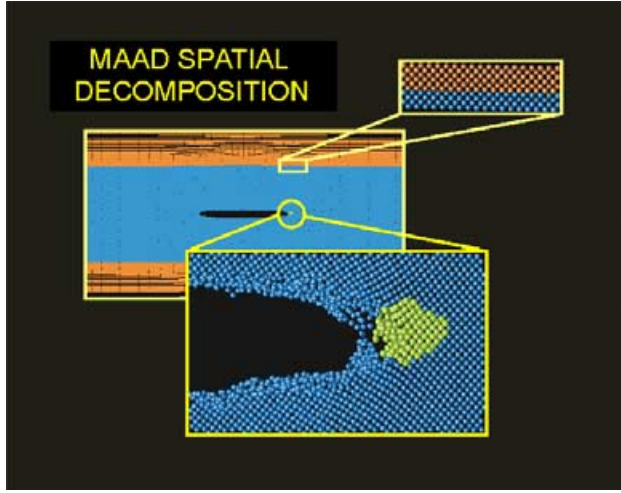


Figure 4 : The geometrical decomposition of the silicon slab into the five different dynamic regions of the MAAD simulation.

Classical Atom Crack Structure

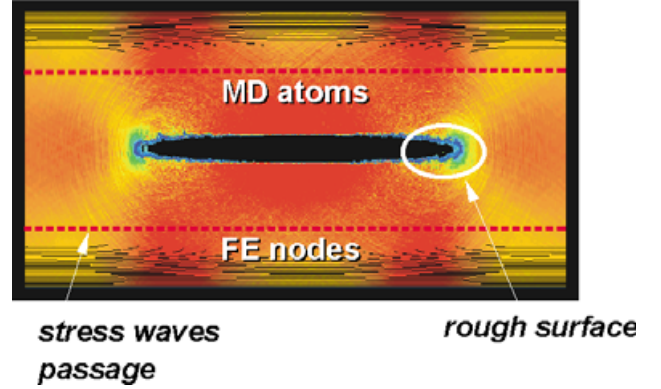


Figure 5 : The stress waves propagating through the slab using a finely tuned potential energy color scale. The crack tips are described by the empirical potential of Stillinger-Weber and are rough with fracture.

Classical and Quantum Atoms

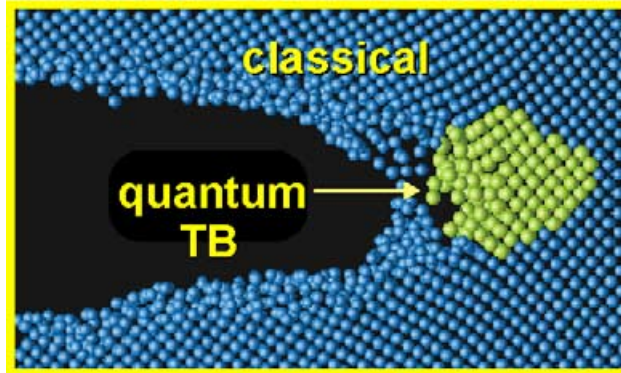


Figure 6 : Constructing the tight-binding (TB) region at the crack tip.

$$\begin{aligned}
 H_{Tot} = & H_{FE}(\{\mathbf{u}, \dot{\mathbf{u}}\} \in FE) + H_{FE/MD}(\{\mathbf{u}, \dot{\mathbf{u}}, \mathbf{r}, \dot{\mathbf{r}}\} \in FE/MD) \\
 & + H_{MD}(\{\mathbf{r}, \dot{\mathbf{r}}\} \in MD) + H_{MD/TB}(\{\mathbf{r}, \dot{\mathbf{r}}\} \in MD/TB) \\
 & + H_{TB}(\{\mathbf{r}, \dot{\mathbf{r}}\} \in TB)
 \end{aligned} \quad (1)$$

This equation should be read as implying that there are three separate Hamiltonians for each sub-system as well as Hamiltonians which dictate the dynamics of variables in the handshake regions. "MD/TB" and "FE/MD" imply such handshake regions. Following a trajectory dictated by this Hamiltonian will result in a conserved total energy.

3 Application to Fracture

In Figure 3, we present the energy-strain relation and the stress-strain relation for bulk silicon as predicted using the SW

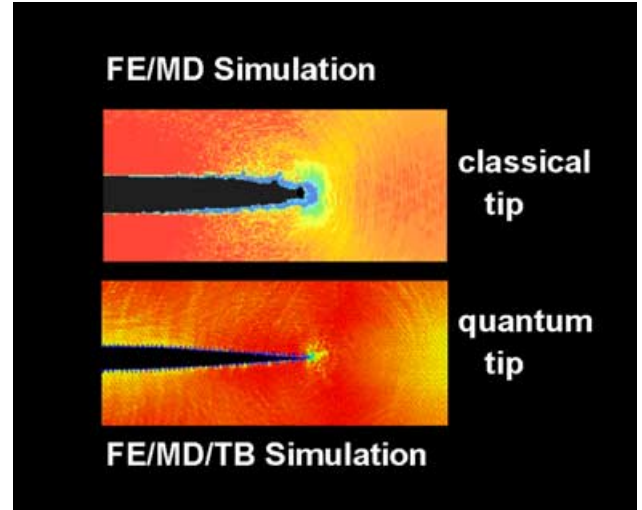


Figure 7 : Crack propagation in silicon using the MAAD method: TB atoms at crack tip, SW atoms surrounding crack, and FE beyond the MD region. The top image shows the system with no tight-binding atoms at the crack tip. The bottom picture shows the brittle fracture via interplanar cleavage for tight-binding atoms at the crack tip region.

empirical potential and the TB method [Abraham, Bernstein, Broughton, , and Hess (2000)]. Uniaxial tension is applied to the bulk silicon with the additional constraint that the interatomic separations change by simple scaling in the stretched direction. The crystal is stretched in the (100) direction. We note that the SW behavior and the TB behavior differs significantly in the hyperelastic regime that governs materials failure at a crack tip. Since the mechanical stability limit occurs at a lower strain using tight-binding, it is reasonable to expect

that a crack tip of TB atoms will fail for a smaller strain than a crack tip of SW atoms. Also, this comparison suggests that the empirical potentials should be fitted to the hyperelastic features of a bulk solid when the interest is to simulate materials failure by empirical potential MD. An important step would be to obtain a reliable data base from accurate quantum mechanical calculations (density functional theory) in the hyperelastic region so that such a program may be carried out. Of course, this would also provide an effective tool for evaluating empirical potentials and tight-binding schemes. For now, we are assuming that our adopted TB scheme is accurate in the hyperelastic regime.

Using MAAD method, we have simulated the fracture of silicon. We create a thin crack in a single crystal silicon samples with either (111) and (100) faces. A system is periodic in the direction perpendicular to the loading direction and crack length. A typical simulated system may have a thickness on the order of 11 Å, and the MD region about 800 Å long in the loading direction and 3500 Å long parallel to the length of the crack. The full system, including the MD and FE regions is about 4000 Å long in the loading direction. The FE region may describe a system *four* times larger than the MD region while increasing the number of degrees of freedom by only 20% and *without significantly increasing the computational effort*. The TB region is moved to remain approximately around the crack tip. The simulation is started by imposing a constant strain rate across the pre-cracked sample.

In Figure 5, we show stress waves propagating through the slab by variations in color that correspond to potential energy variations. The stress waves passing from the MD region to the FE regions show no visible reflection at the FE-MD interface; i.e., the coupling of the MD region with the FE region appears seamless. Both crack tips are characteristic of the fracturing behavior govern by the empirical force law of Stillinger-Weber. We note that the travelling crack's surface are rough and disordered for the crack tips; hence, brittle interplanar cleavage is not observed.

Using the MAAD method by embedding a TB region at the crack tips (Figure 6), we see brittle fracture of silicon proceeding via interplanar cleavage (Figures 7 and 8). For the initial crack length chosen, the TB crack tip starts propagating at a bulk strain of 3.5 percent while a SW crack tip requires a bulk strain above eight percent, consistent with the stress-strain behaviors in Figure 5. Unlike the tight-binding brittle cleavage, the empirical-potential molecular dynamics simulates a blunting crack accompanied by significant atomic disorder. Using the MAAD simulation method, we have simulated the brittle fracture of silicon proceeding via interplanar cleavage.

We have chosen an *ideal* problem, brittle fracture, applied to an *ideal* system, silicon, to illustrate the MAAD simulation approach to *spanning the length scales*. Further applications are being pursued, including dynamical apportioning of TB processors to multiple regions of the physical system (e.g.,

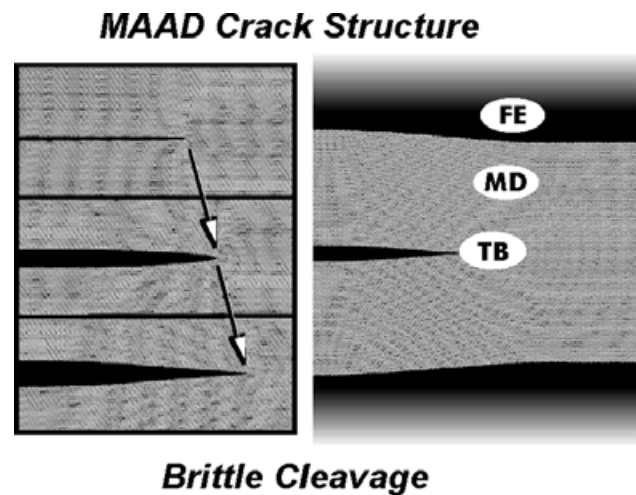


Figure 8 : Time sequence showing the brittle fracture of silicon via interplanar cleavage for the MAAD simulation which incorporates FE/MD/TB.

if crack branching occurs). We wish to emphasize that although progress has been achieved, we view our effort as a beginning to a new and obviously challenging endeavor where improved techniques for the three mechanics will be applied, where more robust procedures for interfacing the three regimes will be invented, and where applications will only be limited by the imagination of the researcher.

References

- Abraham, F. F.; Bernstein, N.; Broughton, J. Q.; ; Hess, D.** (2000): Dynamic fracture of silicon: concurrent simulation of quantum electrons, classical atoms, and the continuum solid. *Materials Research Society Bulletin*, vol. 25, pp. 27–32.
- Abraham, F. F.; Brodbeck, D.; Rafey, R.; Rudge, W. E.** (1994): Instability dynamics of fracture: a computer simulation investigation. *Phys. Rev. Lett.*, vol. 73, pp. 272–275.
- Abraham, F. F.; Broughton, J. Q.; Bernstein, N.; Kaxiras, E.** (1998): Spanning the length scales in dynamic simulation. *Computers In Physics*, vol. 12, pp. 538.
- Abraham, F. F.; Broughton, J. Q.; Berstein, N.; Kaxiras, E.** (1998): Spanning the continuum to quantum length scales in a dynamic simulation of brittle fracture. *Europhysics Letters*, vol. 44, pp. 783.
- Abraham, F. F.; Schneider, D.; Land, B.; Lifka, D.; Skovira, J.; Gerner, J.; Rosendrantz, M.** (1997): Instability dynamics in three-dimensional fracture: an atomistic approach. *J. Mech. Phys. Solids*, vol. 45, pp. 1461–1471.

Bernstein, N.; Kaxiras, E. (1997): Nonorthogonal tight-binding hamiltonian for defects and interfaces in silicon. *Phys. Rev.*, vol. B56, pp. 10488–10496.

Broughton, J. Q.; Abraham, F. F.; Berstein, N.; Kaxiras, E. (1999): Concurrent coupling of length scales: methodology and application. *Phys. Rev. B.*, vol. 60, pp. 2391.

Capaz, R.; Cho, K.; Joannopoulos, J. (1995): Signatures of bulk and surface arsenic antisite defects in gaas(110). *Phys. Rev. Lett.*, vol. 75, pp. 1811–1814.

Clementi, E. (1988): Global scientific and engineering simulations on scalar, vector and parallel LCAP-type supercomputers. *Phil. Trans. Roy. Soc.*, vol. A326, pp. 445–470.

Cottrell, A. H. (1964): *The Mechanical Properties of Matter*. Wiley, New York.

Freund, L. B. (1990): *Dynamical Fracture Mechanics*. Cambridge Univ. Press, New York.

Hoover, W. G.; De Groot, A.; Hoover, C. (1992): Massively parallel computer simulation of plane-strain elastic-plastic flow via nonequilibrium molecular dynamics and lagrangian continuum mechanics. *Computers In Physics*, vol. 6, pp. 155–167.

Hughes, T. (1987): *The Finite Element Method*. Prentice-Hall Inc., New Jersey.

Rafii-Tabar, H.; Hua, L.; Cross, M. (1998): A multiscale atomistic-continuum modelling of crack propagation in a two-dimensional macroscopic plate. *J. Phys.: Cond. Matter*, vol. 10, pp. 2375–2387.

Shenoy, V.; Miller, R.; Tadmor, E.; Phillips, R. (1998): Quasicontinuum models of interfacial structure and deformation. *Phys. Rev. Lett.*, vol. 80, pp. 742–745.

Stillinger, F. H.; Weber, T. A. (1985): Computer simulation of local order in condensed phases of silicon. *Phys. Rev.*, vol. B31, pp. 5262–5271.

Tuckerman, M.; Berne, B. J.; Martyna, G. J. (1990): *J. Chem. Phys.*, vol. 97.

Vanduijnen, P.; Devries, A. H. (1996): Direct reaction field force field: A consistent way to connect and combine quantum-chemical and classical descriptions of molecules. *Int. J. Quant. Chem.*, vol. 60, pp. 1111–1132.

